Tropospheric Ozone and Biomass Burning

S. Chandra, J. R. Ziemke, and P. K. Bhartia
Code 916: NASA Goddard Space Flight Center, Greenbelt, MD 20771

Abstract. This paper studies the significance of pyrogenic (e.g., biomass burning) emissions in the production of tropospheric ozone in the tropics associated with the forest and savanna fires in the African, South American, and Indonesian regions. Using aerosol index (AI) and tropospheric column ozone (TCO) time series from 1979 to 2000 derived from the Nimbus-7 and Earth Probe TOMS measurements, our study shows significant differences in the seasonal and spatial characteristics of pyrogenic emissions north and south of the equator in the African region and Brazil in South America. In general, they are not related to the seasonal and spatial characteristics of tropospheric ozone in these regions. In the Indonesian region, the most significant increase in TCO occurred during September and October 1997, following large-scale forest and savanna fires associated with the El Niño-induced dry season. However, the increase in TCO extended over most of the western Pacific well outside the burning region and was accompanied by a decrease in the eastern Pacific resembling a west-to-east dipole about the dateline. The net increase in TCO integrated over the tropical region between 15°N and 15°S was about 6-8 Tg (1 Tg = 10^{12} gm) over the mean climatological value of about 72 Tg. This increase is well within the range of interannual variability of TCO in the tropical region and does not necessarily suggest a photochemical source related to biomass burning. The interannual variability in TCO appears to be out of phase with the interannual variability of stratospheric column ozone (SCO). These variabilities seem to be manifestations of solar cycle and quasi-biennial oscillations.

Introduction

It is generally recognized that pyrogenic (e.g., biomass burning) emissions produced by the forest and savanna fires in southern Africa and Brazil is a significant source of ozone-producing precursor gases which may produce 10-15 DU (Dobson unit) increases in tropospheric column ozone (TCO) in the south Atlantic region during austral spring [e.g, Fishman et al., 1996, Thompson et al. 1996, Jacob et al., 1996 and several related papers in the special issue of Journal of the Geophysical Research, *101,*1996]. However, recent studies based on 3D atmospheric chemistry and transport models suggest that the photochemical O_3 formation from biomass burning is less important than was indicated in previous studies [e.g., Lelieveld and Dentener, 1999; Marufu et al., 2000, Moxim and Levy, 2000]. The significance of biomass burning in producing TCO was recently discussed by Ziemke and Chandra [1999] based on 20 years (1979-1998) of TCO time series derived from the convective cloud differential (CCD) method using total ozone mapping spectrometer (TOMS) measurements. Their study showed that the amplitude of the annual cycle in the south Atlantic region peaks at about the same time (September and October) from 15° N to 15° S even though the biomass burning in the African region occurs at different times over north and south of the equator. Such a phase lag was not observed following the large scale burning of forest fires in the tropical rainforest of Kalimantan and Sumatra during the El Niño of 1997-98. During September of 1997, when the forest fires were most intense in this region, the TCO increased to about 40-50 DU without any significant phase lag [Chandra et al., 1998; Ziemke and Chandra, 1999]. These values were comparable to values usually observed in the south Atlantic region. In fact the increase in TCO after the Indonesian fires was not limited to this region but extended over thousands of kilometers from the southern part of India in the northern hemisphere to Fiji in the south, and far eastward to Samoa in the southeast, east of the dateline. The question if such a widespread increase in TCO was caused by forest fires over Kalimantan and Sumatra covering a relatively small area of about 45,600 km^2 or by changes in large-scale transport induced by the 1997 El Niño is of considerable importance in understanding the significance that biomass burning has in the photochemical formation of O_3 in the troposphere.

The effect of Indonesian fires on tropospheric ozone was estimated by Hauglustaine et al. [1999] using a global chemical transport model. Using emission rates of ozone precursor gases given by Levine et al. [1999], they estimated in increase of 20-25 DU in TCO over source regions (Sumatra and Kalimantan), in general agreement with the estimates given by Chandra et al. [1998]. However, the estimated ozone amount outside the source region was significantly lower. It is difficult to estimate the temporal and long range implications of these calculations since dynamical conditions prevailing during the El Niño of 1997 was not taken into account.

Using meteorological conditions prevailing during 1997, Sudo et al. [2000] studied the effect of the 1997 El Niño event on tropospheric ozone using a 3D photochemical model developed at the Center for Climate System Research, University of Tokyo, Japan. They were able to simulate most of the observed changes in tropospheric ozone reported by Chandra et al. [1998] and concluded that the both the biomass burning and the changes in meteorological conditions (e.g., low convective activity, sparse precipitation, dry air condition, enhanced transport from the stratosphere) contributed almost equally to the observed enhancement in tropospheric ozone in the Indonesian region.

The 1997 El Niño event was unique since the forest fires in Indonesia were preceded by the burning seasons in Brazil and southern Africa. The purpose of this paper is to study the possible role of these events on tropospheric ozone which was significantly elevated for several months over half the tropical belt encompassing South America, Southern Africa and Indonesia. Our study is based on TCO derived from the CCD method [Ziemke et al., 1998] and ozone profiles derived from ozonesondes from a number of tropical stations. These sondes have been operating under the SHADOZ (Southern Hemisphere Additional Ozonesondes) program which was initiated by NASA/Goddard Space Flight Center in 1998 with the participation of a number of US and international investigators [Thomson and Witte, 1999]

The biomass burning events are inferred from the aerosol smoke index (AI) which is calculated from the ratio of a pair of ultraviolet wavelengths measured from TOMS instruments as follows [Hsu et al., 1996]:

$$AI = -100[\log_{10}(I_{340}/I_{380})_{meas} - \log_{10}(I_{340}/I_{380})_{calc}], \qquad (1)$$

where $(I_{340}/I_{380})_{meas}$ is the ratio of the backscattered radiances at 340 and 380 nm measured by TOMS and $(I_{340}/I_{380})_{calc}$ is the corresponding values calculated from a radiative transfer model for a pure Rayleigh-scattering atmosphere. The positive and negative values of AI generally correspond to absorbing and non-absorbing aerosols at UV wavelengths, respectively. The wavelengths used in (1) applies to Nimbus 7 TOMS measurements. For the Earth Probe TOMS instrument the 340 nm wavelength is replaced by 331 nm, and 380 nm is replaced by 360 nm.

Both the CCD and AI data used in this study are monthly averages with a horizontal resolution of 5° by 5° within the latitude range 15°S to 15°N (centered on latitudes 12.5°S, 7.5°S, ..., 12.5°N). There is a large gap of missing CCD and AI data from May 1993 through June 1996 because there were no applicable TOMS satellite measurements during this time period. Although the Meteor-3 TOMS instrument made measurements from late August 1991 to December 1994, the non-sun-synchronous orbit of the satellite created high solar zenith angles in the tropics which generated a large amount of spurious CCD TCO measurements. The CCD data used in this study had several corrections including adjustments for tropospheric aerosols, a

partial correction for sea glint errors, an ozone retrieval efficiency correction for the lower troposphere, and an instrument calibration offset correction between Nimbus 7 and Earth probe TOMS. Details on these corrections are discussed by Ziemke et al. [2000] and Ziemke et al. [2001].

TCO and AI Climatologies

Plate 1 shows the zonal variation in AI (left) and TCO (right) climatology in the tropics based on 22 years of data from 1979 through 2000. The four panels on each side are averages of the months December-January-February (DJF), March-April-May (MAM), June-July-August (JJA), and September-October-November (SON). These seasonal averages represent winter (summer), spring (fall), summer (winter), and fall (spring) conditions of the northern (southern) hemisphere. The seasonal and zonal characteristics of TCO inferred from Plate 1 are similar to the ones discussed in Ziemke and Chandra [1999]. Plate 1 shows a predominantly zonal wavenumber 1 feature in all seasons with maximum in the Atlantic and minimum in the Pacific region. The seasonality in the Pacific region is generally weak, and is stronger in the Atlantic region with minimum in MAM and maximum in SON seasons. The amplitude of the seasonal cycle in the Atlantic region increases from 3 DU north of the equator to around 6 DU south of equator. Assuming that AI values less than 0.6 are not statistically significant [e.g., Hsu et al., 1999], Plate 1 suggests that the African region is the major source of aerosols. Unfortunately the AI measurement does not always indicate the presence of carbonaceous aerosol produced by biomass burning. Hsu et al. [1999] showed that the derived AI is linearly proportional to aerosol optical thickness (AOT) derived independently from ground-based sun-photometers over regions of biomass burning and regions covered by African dust. However, their study suggests that the high values of AI (>0.7) in summer (Plate 1, third panel) are caused by savanna burnings in southern Africa. In northern Africa, high values of AI (Plate 1, first and second panels) are associated with both the desert dust and biomass burning. This picture is generally consistent with the monthly-mean fire count map derived from the ATSR-2 night images (http://shark1.esrin.esa.it/ionia/FIRE/AF/ATSR). Plate 1 suggests an apparent relation between AI and TCO south of the equator in the southern African region. TCO increased at about the same time as AI. However, TCO continued to increase over a much wider region extending to South America in the west and Indian Ocean in the east well after the burning stopped.

In general, TCO peaks in September-October, about 2 months after AI reaches peak values around July-August over most of the regions in southern Africa. Figure 1 compares monthly fluctuations in AI and TCO at Nairobi, Kenya (1°S, 37°E), a city situated near the equator in the African region, but outside the burning region as inferred from AI measurements

for this location as well as the source region located at about 30-35 degree west of Kenya (Plate 1). All these time series cover the time period of EP TOMS measurements beginning from August 1996 to the end of 2000. Figure 1 also compares the TCO time series derived from the CCD method with TCO derived from ozonesonde at Nairobi over the two year period (1997-1999) when the two measurements overlap. The two time series are in remarkable agreement both with respect to their absolute values and temporal changes. They both show strong seasonal cycles with peak values of about 40 DU during September-October months. AI in the source region has a similar seasonal behavior but with peak values in July and August. Such a phase relation is not indicated in regions north of the equator.

AI in northern Africa is strongly influenced by desert mineral dust from Saharan and Sahel dust storms and does not necessarily indicate the presence of carbonaceous aerosols. Relatively high vlaues of TCO from the western coast of Africa to the eastern coast of South America (Plate 1, upper panel) thus does not seem to be related to biomass burning. Thompson et al. [2000] have characterized this apparent anomaly as the 'tropical Atlantic paradox'. One may arrive at a similar conclusion about the possible effect of biomass burning on TCO in Brazil (Plate 1, lower panels). The climatological values of AI in this region when averaged over the three-month SON period is not statistically significant even though the TCO field over the same period is almost as robust as over the African region. These results clearly suggest that the effect of biomass burning on tropospheric ozone in the tropics is not as large as generally believed. They are however consistent with recent calculations by Marufu et al. [2000] based on a global chemical transport model. Marufu et al. [2000] have shown that the pyrogenic (e.g., biomass burning) emissions accounted for only 16% of tropospheric ozone produced in the African region. The remaining contributions came from emissions from industrial, biogenic, lightning, and stratospheric influx, with numbers of 19%, 12%, 27%, and 26%, respectively.

TCO field during 1997 El Niño

The basic pattern of TCO and AI fields shown in Plate 1 do not change significantly from year-to-year except during El Niño years which are accompanied by a change in the convection pattern and biomass burning in the Indonesian region. This is seen in plate 2 which shows AI and TCO fields for 1997-1998 El Niño. The two fields are very similar to climatological fields as in plate 1 except in the Indonesian region. The latter shows a significant increase in AI during September and October encompassing the islands of Sumatra and Borneo (plate 2 left, fourth panel) associated with the biomass burning in this region. The corresponding increase in TCO after the Indonesian fires is not limited to this region but extends over thousands of kilometers from southern India in the north, to Fiji in the south, and eastward as far as Samoa. A detailed

analysis of these observations suggest that in spite of an apparent correlation of AI and TCO in the Indonesian region, most of the increase in TCO is a manifestation of large scale circulation processes associated with the shift in the tropical convection pattern.

Plates 3-7 show zonal variations in AI and TCO in the tropics for years preceding (1996), during (1997), and after (1998) the El Niño episode which developed during March 1997 and strengthened rapidly over several months after that. To highlight the effect of tropical convection the orientations of these plates, with respect to plate 1, are shifted by 180 with the dateline (180° longitude) in the middle. Plate 3 shows these fields for the month of August. August 1997 preceded the onset of large scale forest fires during September and October 1997 in the Indonesian region (Plates 4 and 5). The AI field in plate 3 shows significant enhancement (>0.7) over a very large area in southern Africa and a similar increase in Brazil in South America but over a much smaller area. These increases are associated with the biomass burning in these regions. Though the general pattern of the AI field is similar in all three years, the TCO field in 1997 (plate 3, middle panel) is significantly different compared to the preceding and the later years. The TCO field in August in all three years shows a characteristic wave 1 pattern with high values of 30-40 DU in the southern Atlantic region and low values in the Pacific region. During August 1997 the low region was shifted east of the dateline causing a decrease of 6-8 DU over most of the eastern Pacific region. An increase of about the same magnitude occurred over regions of the western Pacific including Indonesia. These positive and negative changes were almost entirely due to the shift in the convection pattern from the western to the eastern Pacific and the related changes in the tropical circulation as discussed in Chandra et al. [1998]. With the intensification of El Niño, the Indonesian region showed a rapid buildup of ozone over a considerably larger area than affected by forest fires (e.g., plates 4 and 5, middle panels). As seen in plates 6 and 7 (middle panels) the zonal contrast in TCO persisted over several months with significantly high values of TCO (40-50 DU) in the western Pacific well after the cessation of forest fires in the Indonesian region. For the biomass burning to be an effective source of TCO, the ozone precursors (NO_x, CO, and hydrocarbons) produced during forest fires have to be transported rapidly from the lower to the middle troposphere. This is not a likely mechanism in regions of suppressed convection and is not supported by spatial and temporal measurements of these constituents by ozonesonde and aircraft in this region as will now be discussed.

Figure 2 shows relative variations of TCO and AI at Watukosek (8°S, 113°E) in eastern Java from 1996 to 2000. Watukosek is just outside the region of intense biomass burning as indicated from the temporal variations of AI at this location and Kalimantan (3°S, 113°E) which is about 5 degrees north of Watukosek. The ozonesonde data at Watukosek with respect to 1997 El Niño has been discussed in detail by Fujiwara et al. [1999, 2000] and can be compared directly with overlapping CCD measurements. The CCD derived ozone at Watukosek seems to

be in good agreement with the ozonesonde data. Both of these measurements suggest that the peak values in TCO reached during September-October 1997 occurred about one to two months after the peak in AI. This increase is about 15-20 DU compared to a mean value of about 30 DU during October 1996 and, as in Plate 5, cannot be attributed to local production of ozone and ozone precursors in the lower troposphere. Analysis of ozone profiles from ozonesonde data at Watukosek suggests that most of the increase in TCO during 1997 comes primarily from regions above 3 km [Fujiwara et al., 2000]. The integrated column ozone between 0-3 km did not change significantly from 1996 to 1997. There is no indication that biomass burning caused a significant increase in the lower troposphere even in the source region. The aircraft measurements of ozone and ozone precursors (NO_X and CO) during October 1997 over Kalimantan showed very high values CO mixing ratio (3 to 9 ppm) below 2.6 km but very low values of NO_X/CO ratio (0.0002 to 0.0005) compared to background values [Sawa et al., 1999]. Tsutsumi et al. [1999] have shown that over Kalimantan, both aerosol and NO_X decreased with altitude. However, ozone had an opposite trend with very low concentrations (~20 ppbv) in the lower smoke layer and high concentrations (~80 ppbv) in the middle troposphere [Tsutsumi et al.,1999]. These measurements suggest that the effect of ozone producing precursors was not very significant during Indonesian fires. The reduction in NO_X emissions during Indonesian fires is particularly noteworthy since NO_X is the reaction limiting species in the photochemical production of tropospheric ozone.

As seen in plates 3-7 the TCO values in regions near the date line did not change significantly from the non-El Niño to El Niño years. This is also reflected in the ozonesonde data at Samoa (14°S, 171°W) which is located in the south Pacific region. Figure 3 compares TCO measured from ozonesondes with CCD-derived TCO at Samoa over the 1996-1998 time period. As in Figures 1 and 2, TCO derived from the two sets of measurement at this location are in good agreement and show similar seasonal and temporal variations within the uncertainty of the two sets of measurements. The seasonal cycles during 1996 and 1998 are essentially similar showing a steep rise from about 10-15 DU to about 20-25 DU during the early part of the year. In comparison 1997 appears to be more noisy which may be attributed to El Niño induced shifts in the transition region.

Dynamical Implications

The possible role of large-scale transport on tropospheric ozone can best be studied using a global 3D photochemical and transport model. This is illustrated in Plate 8 which compares the observed and simulated changes in tropospheric ozone related to 1997 El Niño. The later is based on a 3 D photochemical and transport model using meteorological conditions prevailing

during 1997 [Kengo Sudo, personal communicaton, 2000; Sudo et al., 2000]. The model was run with and without biomass burning sources. Plate 8 compares observed ozone anomalies during October 1997 for a simulation without biomass burning sources. The latter reproduces the observed features remarkably well, at least qualitatively. Both the observed and simulated changes in TCO show a dipole structure as discussed in Chandra et al. [1998] with a positive anomaly in O_3 extending well outside of the Indonesian region. The peak values of the observed anomaly (16-20 DU) are higher than the model values (12-14 DU) by 4-6 DU but are within the range of both the model and observational uncertainty. However, an increase of this magnitude may also have been caused by photochemical production of ozone caused by biomass burning in the Indonesian region.

Since transport related changes in the tropics produce both positive and negative anomalies, they tend to cancel each other in the zonally averaged data. It is therefore useful to integrate TCO over the tropical region and estimate the net increase in TCO attributed to photochemical sources. Figure 4 compares the seasonal variation in TCO over the tropical region in 1997 with a climatology based on the 21 years (1979-1999) of CCD data base. Both data sets are area-averaged over the latitude band from 15°N to 15°S and are expressed in the units of terra-grams (Tg; 1 Tg = 10^{12} gm) to reflect the ozone mass abundance in the tropical troposphere. Figure 4 indicates a clear seasonal pattern in TCO climatology with a mean value of about 72 Tg . This is about 3 times larger than the TCO abundance in the African region estimated by Marufu et al. [2000]. The TCO climatology has a relatively weaker peak in spring and a stronger peak in fall. These peaks are reflections of higher values of ozone in these months over the tropical Atlantic region encompassing most of southern Africa and Brazil (Plate 1). Compared to climatology, the TCO values over most of 1997 are elevated after the development of El Niño in March 1997. However, the elevated values do not necessarily mean presence of photochemical sources associated with biomass burning in the Indonesian region. For example, during September and October 1997 when the biomass burning was most intense in the Indonesian region (Plates 5 and 6), the TCO values were 10-15 Tg higher than climatology. A critical point is that these values are comparable to a similar enhancement seen during June and July 1997, long before the start of large-scale forest fires in the Indonesian region.

A time series analysis of zonally averaged TCO in the tropics suggests that the 1997 increase in TCO is mostly a manifestation of interannual variability in the troposphere associated with a change in large-scale transport. Figure 5 shows the interannual variability in TCO with respect to its climatology over the 1979-1999 period. Shown in this figure is also the corresponding interannual variability in SCO (stratospheric column ozone). Both the time series show monthly fluctuations with respect to their climatologies. They are area-averaged over 15°N to 15°S (as in Figure 4) and smoothed using a 12-month digital lowpass filter to accentuate

changes over a longer (QBO) time scale. Figure 5 shows an increase of about 6-8 Tg during 1997 over mean climatological values of 70-75 Tg. However, this increase is well within the range of interannual variability and does not differ significantly from non-El Niño years. Both the TCO and SCO time series show low frequency oscillations which are characteristic of QBO as inferred from the zonal wind at 30 mb measured at Singapore (not shown). The positive and negative anomalies in SCO tend to follow the westerly and easterly phases of the QBO cycle as inferred from the 30 mb wind at Singapore (not shown). Negative and positive anomalies in TCO tend to follow the easterly and westerly phases of the QBO. In general the TCO variability is out of phase with the SCO variability except during the 1990-1992 period when they tend to be inphase. Some of this inphase discrepancy may be attributed to changes in circulation during 1991-1992 caused by the series of Mt. Pinatubo eruptions. However, there may be other reasons particularly before Pinatubo eruption which are not well understood. Ziemke and Chandra [1999] have shown that the QBO type of oscillations in SCO and TCO time series were persistent over the tropical Atlantic region. Over most of the Pacific region where El Niño induced oscillations were very robust, the effect of QBO was less significant. A strong QBO signal in the tropically averaged data is due to the cancellation of the El Niño effects which induces an west-to-east dipole about the dateline.

Figure 5 also suggests a solar cycle modulation of both the SCO and TCO time series. The two time series are respectively in phase and out of phase with the solar cycle. Evidence for a solar cycle in tropospheric ozone was shown by Chandra et al. [1999] for the marine atmosphere in the tropics. This effect is also present in the zonally averaged data as indicated by significantly larger differences between the zonal anomalies of TCO and SCO time series during solar minimum (1985-1988, 1995-1998) conditions.

The magnitude of QBO and solar cycle components can be estimated using a linear regression model [discussed by Ziemke and Chandra, 1999]. For TCO in Figure 5, the peak-to-peak amplitudes for the QBO and solar cycle components are 5 and 6 Tg, respectively. Assuming a mean value of 72 Tg, this corresponds to a peak-to-peak modulation of about 6% by the QBO and about 8% for the solar cycle. The analysis presented in this section clearly shows that the increase in TCO after the Indonesian fires during 1997 is mostly a manifestation of changes in the circulation pattern in the tropics and does not represent a net increase in TCO produced by biomass burning.

Summary and Conclusions

In this paper we have studied the possible role of biomass burning in producing seasonal and interannual variabilities in tropospheric ozone in the tropics. Using TOMS derived AI as an index of pyrogenic emissions associated with savanna and forest fires, we noted four major regions of significant biomass burning. Two of these regions lie north and south of the equator in the African subcontinent and the other two regions lie in Brazil in South America and Indonesia in South East Asia. The African regions are associated with the dry periods which include December-January-February in the northern part and June-July-August in the southern part of Africa. The Brazilian fires are also associated with the dry season (July-August-September) in Brazil. However, they are not as persistent as the fires in the African regions. These differences may probably be related to the differences in the meteorological conditions of the two regions. Notwithstanding the differences in biomass burning patterns of the three regions, the seasonal changes in TCO in these regions are essentially similar, and in general do not seem to be related to the seasonal changes in AI.

In the Indonesian region, the climatological values of AI are not statistically significant in any season. The most significant increase in AI occurred during September-October of 1997 after the large-scale biomass burning which included both forest fires and Savanna fires. Our study has shown that TCO in this region began to increase before the onset of major fire events and reached peak values of 50-60 DU during September and October of 1997. The elevated values of TCO persisted for several months after the fire events subsided. During the entire El Niño episode, the increase in TCO was not limited to the biomass burning regions of Sumatra and Kalimantan in the Indonesian region but was extended over thousands of kilometers encompassing most of the western Pacific region. The increase in TCO in the western Pacific region was accompanied by a decrease in the eastern Pacific resembling a west-to-east dipole about the dateline. The model calculations suggest that these changes are more a characteristic of dynamically induced changes than the changes induced by biomass burning. The net increase in TCO integrated over the tropical region 15°S to 15°N is about 6-8 Tg over the climatological mean of about 72 Tg. Though some of this increase may have been caused by photochemcial production of ozone related to biomass burning, an increase of this magnitude is well within the range of interannual variability of tropical TCO. An analysis of the interannual variabilities in TCO and SCO time series integrated over tropical latitudes suggest that both the time series are influenced by QBO and solar cycle induced oscillations. The stratospheric and tropospheric oscillations are generally out of phase with respect to each other and clearly suggest a significant role of atmospheric transport.

The conclusions arrived at in this study does not change if one uses fire counts instead of AI as an index of pyrogenic emissions. None of these indices provide quantitative estimates of hydrocarbons and NO_X emissions which are needed for realistic simulations of photochemical

processes. These uncertainities are reflected in current 3D photochemical and transport models as discussed in a number of studies [e.g.,Hauglustaine et al., 1998; Wang et al., 1998, Moxim and Levy, 2000; Marufu et al., 2000]. For example, the contribution of biomass burning to tropospheric ozone estimated by Marufu et al. is only 16 %. compared to 36 % estimated by Moxim and Levy [2000]. The latter estimate a relatively higher contribution from lightning, 49 % compared to 27 % estimated by Marufu et al. The effect of lightning on tropospheric ozone has also been inferred from the EOF (empirical orthogonal function) analysis of the CCD data [Martin et al., 2000]. Our future study will involve detailed comparisons of ozone derived from the CCD and cloud slicing methods [Ziemke et al., 2001] with 3-D photpchemical transport models with realistic simulations of photochemical and transport processes. The importance of comparing model with observational data is two-fold. The models provide valuable insight to understanding the chemistry and dynamics which determine the observed ozone distributions, and the observed data can be used to help identify potential problems in models.

Acknowledgments. We thank Kengo Sudo for providing the model results for 1997 El Niño presented at the XVIV Quadrennial Ozone Symposium at Sapporo, Japan. The ozonesonde data for Watukosek were provided by Shuji Kawakami. We also thank Christina Hsu and Paul Ginoux for helpful discussions.

References

Chandra, S., J. R. Ziemke, W. Min, and W. G. Read, Effects of 1997-1998 El Niño on tropospheric ozone and water vapor, *Geophys. Res. Lett., 25*, 3867-3870, 1998.

Chandra, S., J. R. Ziemke, and R. W. Stewart, An 11-year solar cycle in tropospheric ozone from TOMS measurements, *Geophys. Res. Lett., 26*, 185-188, 1999.

Fishman, J., V. G. Brackett, E. V. Browell, and W. B. Grant, Tropospheric ozone derived from TOMS/SBUV measurements during TRACE A, J. Geophys. Res., 101, 24,069-24,082, 1996.

Fujiwara, M., K. Kita, S. Kawakami, T. Ogawa, N. Komala, S. Saraspriya, and A. Suripto, Tropospheric ozone enhancements during the Indonesian forest fire events in 1994 and in 1997 as revealed by ground-based observations, *Geophys. Res. Lett., 26*, 2417-2420, 1999.

Fujiwara, M., K. Kita, T. Ogawa, S. Kawakami, T. Sano, N. Komala, S. Saraspriya, and A.

Suripto, Seasonal variation of tropospheric ozone in Indonesia revealed by 5-year ground-based observations, *J. Geophys. Res., 105*, 1879-1888, 2000.

Hauglustaine, D. A., G. P. Brasseur, S. Walters, P. J. Rasch, J.-F. Muller, L. K. Emmons, and M. A. Carroll, MOZART, a global chemical transport model for ozone and related chemical tracers, 2, Model results and evaluation, *J. Geophys. Res., 103*, 28,291-28,335, 1998.

Hauglustaine, D. A., Brasseur G. P., and J. S. Levine, A sensitivity simulation of tropospheric ozone changes due to the 1997 Indonesian fire emissions, *Geophys. Res. Lett., 26*, 3305-3308, 1999.

Hsu, N. C., J. R. Herman, P. K. Bhartia, C. J. Seftor, O. Torres, A. M. Thompson, J. F. Gleason, T. F. Eck, and B. N. Holben, Detection of biomass burning smoke from TOMS measurements, *Geophys. Res. Lett., 23*, 745-748, 1996.

Jacob, J., et al., Origin of ozone and NO_X in the tropical troposphere: A photochemical analysis of aircraft observations over the South Atlantic basin, *J. Geophys. Res., 101*, 24,235-24,250, 1996.

Lelieveld, J., and F. J. Dentener, What controls tropospheric ozone?, *J. Geophys., Res., 105*, 3531-3551, 2000.

Levine, J. S., The 1997 fires in Kalimantan and Sumatra, Indonesia: Gaseous and particle emissions, *Geophys. Res. Lett., 26*, 815-819, 1999.

Martin, R. V., D. J. Jacob, J. A. Logan, J. R. Ziemke, and R. Washington, Detection of a lightning influence on tropical tropospheric ozone, *Geophys. Res. Lett., 27*, 1639-1642, 2000.

Marufu, L., F. Dentener, J. Lelieveld, M. O. Andreae, and G. Helas, Photochemistry of the African troposphere: Influence of biomass burning emission, *J. Geophys. Res., 105*, 14,513-14,530, 2000.

Moxim, W. J., and H. Levy II, A model analysis of tropical South Atlantic Ocean tropospheric ozone maximum: The interaction of transport and chemistry, *J. Geophys. Res., 105*, 17,393-17,415, 2000.

Sawa, Y., H. Matsueda, Y. Tsutsumi, J. B. Jensen, H. Y. Inoue, and Y. Makino, Tropospheric carbon monoxide and hydrogen measurements over Kalimantan in Indonesia and northern Australia during October, 1997, *Geophys. Res. Lett., 26*, 1389-1392, 1999.

Sudo, K., M. Takahashi, and H. Akimoto, Development of a photochemical GCM for the troposphere: Some experiments on the tropospheric ozone change, *XVIV Quad. Ozone Symp.*, 181-182, Sapporo, 2000.

Thompson, A. M., K. E. Pickering, D. P. McNamara, M. R. Schoeberl, R. D. Hudson, J. H. Kim, E. V. Browell, W. W. J. H. Kirchhoff, and D. Nganga, Where did tropospheric ozone over southern Africa and the tropical Atlantic come from in October 1992?, Insights from TOMS, GTE/TRACE-A and SAFARI-92, *J. Geophys. Res., 101*, 24,251-24,278, 1996.

Thompson, A. M., B. G. Doddridge, J. C. Witte, R. D. Hudson, W. T. Luke, J. E. Johnson, B. J. Johnson, S. J. Oltmans, R. Weller, A tropical Atlantic paradox: Shipboard and satellite views of the tropospheric ozone maximum and wave-one in January-February 1999, *Geophys. Res. Lett., 27*, 3317-3320, 2000.

Thomson, A. M., J. C. Witte, SHADOZ (Southern Hemisphere Additional Ozonesondes): A new ozonesonde data set for the Earth Science Community, *Earth Observer, 11(4)*, 27-30, 1999.

Tsutsumi, Y., Y. Sawa, Y. Makino, J. B. Jensen, J. L. Gras, B. F. Ryan, S. Diharto, and H. Harjanto, Aircraft measurements of ozone, NO_X, CO, and aerosol concentrations in biomass burning smoke over Indonesia and Australia in October 1997: Depleted ozone layer at low altitude over Indonesia, *Geophys. Res. Lett., 26*, 595-598, 1999.

Wang, Y.l, D. J. Jacob, and J. A. Logan, Global simulation of tropospheric O_3-NO_X-hydrocarbon chemistry, 1, Model formulation, *J. Geophys. Res., 103*, 10,713-10,725, 1998.

Ziemke, J. R., S. Chandra, and P. K. Bhartia, Two new methods for deriving tropospheric column ozone from TOMS measurements: The assimilated UARS MLS/HALOE and convective-cloud differential techniques, *J. Geophys. Res., 103*, 22,115-22,127, 1998.

Ziemke, J. R., and S. Chandra, Seasonal and interannual variabilities in tropical tropospheric ozone, *J. Geophys. Res., 104*, 21,425-21,442, 1999.

Ziemke, J. R., S. Chandra, and P. K. Bhartia, A new NASA data product: Tropospheric and stratospheric column ozone in the tropics jderived from TOPMS meaurements, *Bull. Amer. Meteorol. Soc., 81*, 580-583, 2000.

Ziemke, J. R., S. Chandra, and P. K. Bhartia, Cloud slicing: A new technique to derive upper tropospheric ozone from satellite measurements, *J. Geophys. Res.*, in press, 2001.

Figure Captions

Figure 1. Tropospheric total column O_3 at Nairobi (1°S, 37°E) derived from ozonesonde (stars) and CCD method (solid) . Also plotted along the bottom of the figure is the TOMS aerosol index time series at Nairobi (dashed) and at 7.5°S, 7.5°E (dotted). The aerosol index time series at 7.5°S, 7.5°E is centered about the region of largest detected smoke from biomass burning over western and southern Africa (see aerosol index data in Plate 1 for JJA season). Vertical bars for the ozonesonde data represent $\pm 1\sigma$ standard deviations.

Figure 2. Tropospheric total column O_3 at Watukosek (8°S, 113°E) derived from ozonesonde (stars) and CCD method (solid) . Also plotted along the bottom of the figure is the TOMS aerosol index time series at Watukosek (dashed) and at 2.5°S, 112.5°E (dotted). The aerosol index time series at 2.5°S, 112.5°E is centered about the region of largest detected smoke from biomass burning over Indonesia during the 1997-1998 El Niño (see tropospheric ozone data in Plate 2 for the 1997 SON season). Vertical bars for the ozonesonde data represent $\pm 1\sigma$ standard deviations.

Figure 3. Tropospheric total column O_3 at Samoa (14°S, 171°W) derived from ozonesonde (stars) and CCD method (solid) . Vertical bars for the ozonesonde data represent $\pm 1\sigma$ standard deviations.

Figure 4. Tropospheric total ozone mass abundance (units Tg) time series derived by area-averaging CCD tropospheric total column O_3 in the latitude band 15°S to 15°N for 1997 (dotted) and a 1979-2000 climatology (solid). Vertical bars represent $\pm 2\sigma$ uncertainties.

Figure 5. Tropospheric (thick solid) and stratospheric (thin solid) total ozone mass abundance (units Tg) deseasonalized time series derived by area-averaging CCD column O_3 measurements in the latitude band 15°S to 15°N. The original deseasonalized monthly mean data (dotted and dashed curves) were smoothed with a digital recursive low-pass filter with half frequency response at 12-month period.

Plate 1. Left: TOMS aerosol index (no units) seasonal climatology. The data shown were determined by averaging over 3-month seasons (indicated) for the time period 1979-2000. Bottom: Same as the left-hand frames, but for TOMS CCD tropospheric total column ozone (in Dobson units).

Plate 2. Same as Plate 1, but for the year 1997 instead of climatology.

Plate 3. Left: TOMS aerosol index (no units) for August 1996 (top), August 1997 (middle), and August 1998 (bottom). Right: Same as left-hand frames, but for TOMS CCD tropospheric total column O_3 (in Dobson units). The dateline (in contrast to Plates 1 and 2) is now shown in the middle of each frame.

Plate 4. Same as Plate 3, but for September 1996-1998

Plate 5. Same as Plate 3, but for October 1996-1998

Plate 6. Same as Plate 3, but for November 1996-1998.

Plate 7. Same as Plate 3, but for December 1996-1998

Plate 8. Top: TOMS CCD tropospheric total column O_3 anomaly field for October 1997. The anomaly field was derived by subtracting a 1979-2000 year climatology from the original October 1997 CCD data. The dateline is shown in the middle of the frame. Bottom: Similar to CCD anomaly field in top frame, but instead for a 3D photochemical transport model with a model climatology [Sudo et al., 2000].

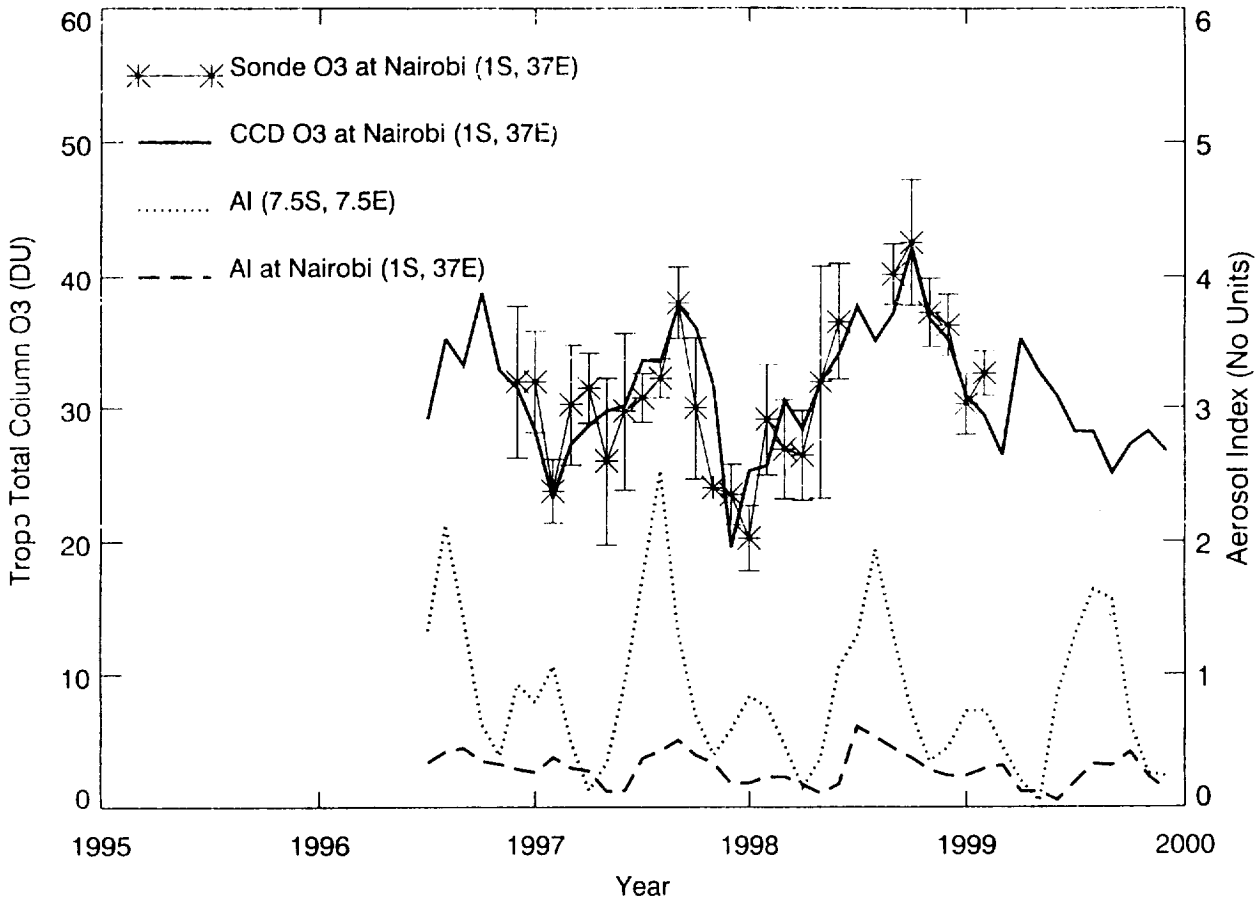

Figure 1. Tropospheric total column O_3 at Nairobi (1°S, 37°E) derived from ozonesonde (stars) and CCD method (solid) . Also plotted along the bottom of the figure is the TOMS aerosol index time series at Nairobi (dashed) and at 7.5°S, 7.5°E (dotted). The aerosol index time series at 7.5°S, 7.5°E is centered about the region of largest detected smoke from biomass burning over western and southern Africa (see aerosol index data in Plate 1 for JJA season). Vertical bars for the ozonesonde data represent $\pm 1\sigma$ standard deviations.

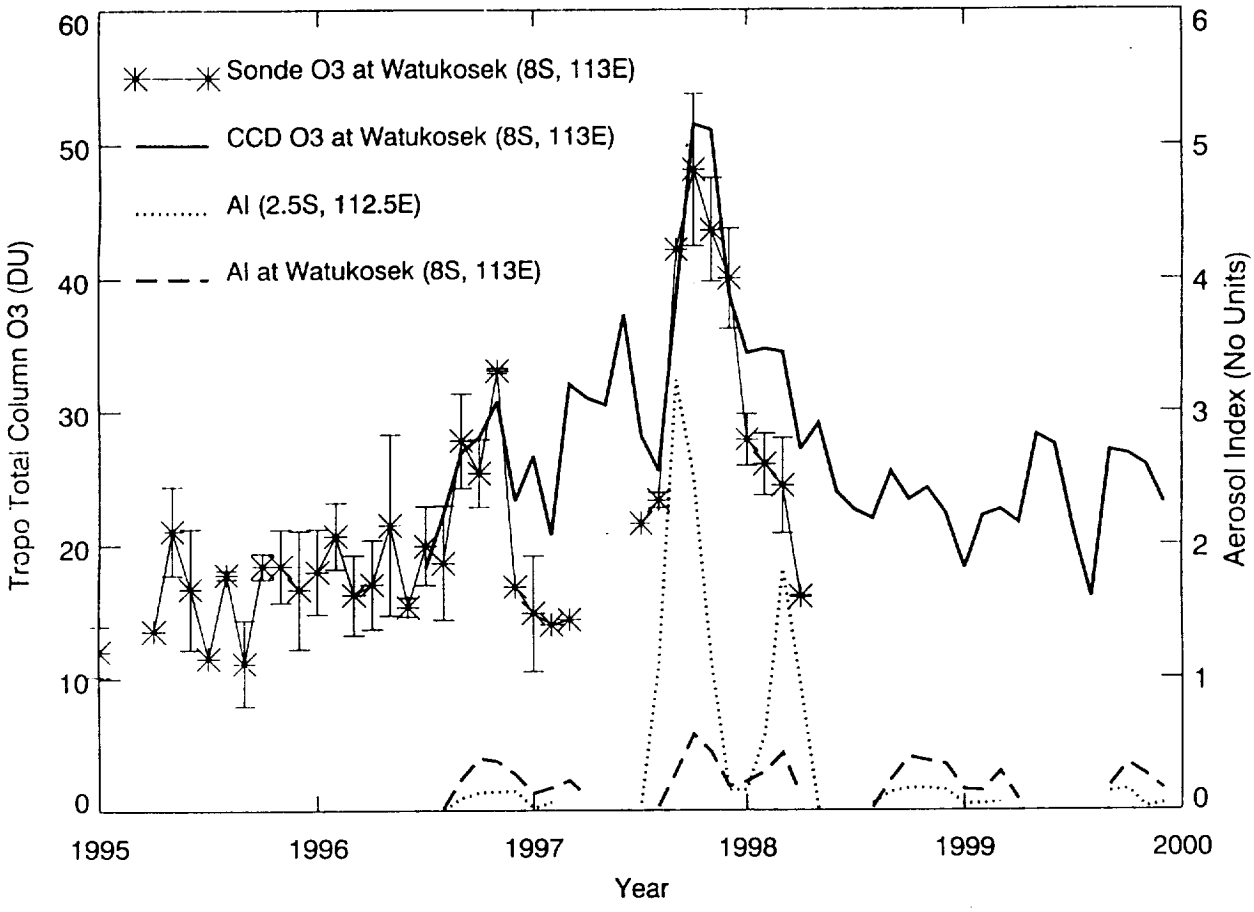

Figure 2. Tropospheric total column O_3 at Watukosek (8°S, 113°E) derived from ozonesonde (stars) and CCD method (solid) . Also plotted along the bottom of the figure is the TOMS aerosol index time series at Watukosek (dashed) and at 2.5°S, 112.5°E (dotted). The aerosol index time series at 2.5°S, 112.5°E is centered about the region of largest detected smoke from biomass burning over Indonesia during the 1997-1998 El Niño (see tropospheric ozone data in Plate 2 for the 1997 SON season). Vertical bars for the ozonesonde data represent $\pm 1\sigma$ standard deviations.

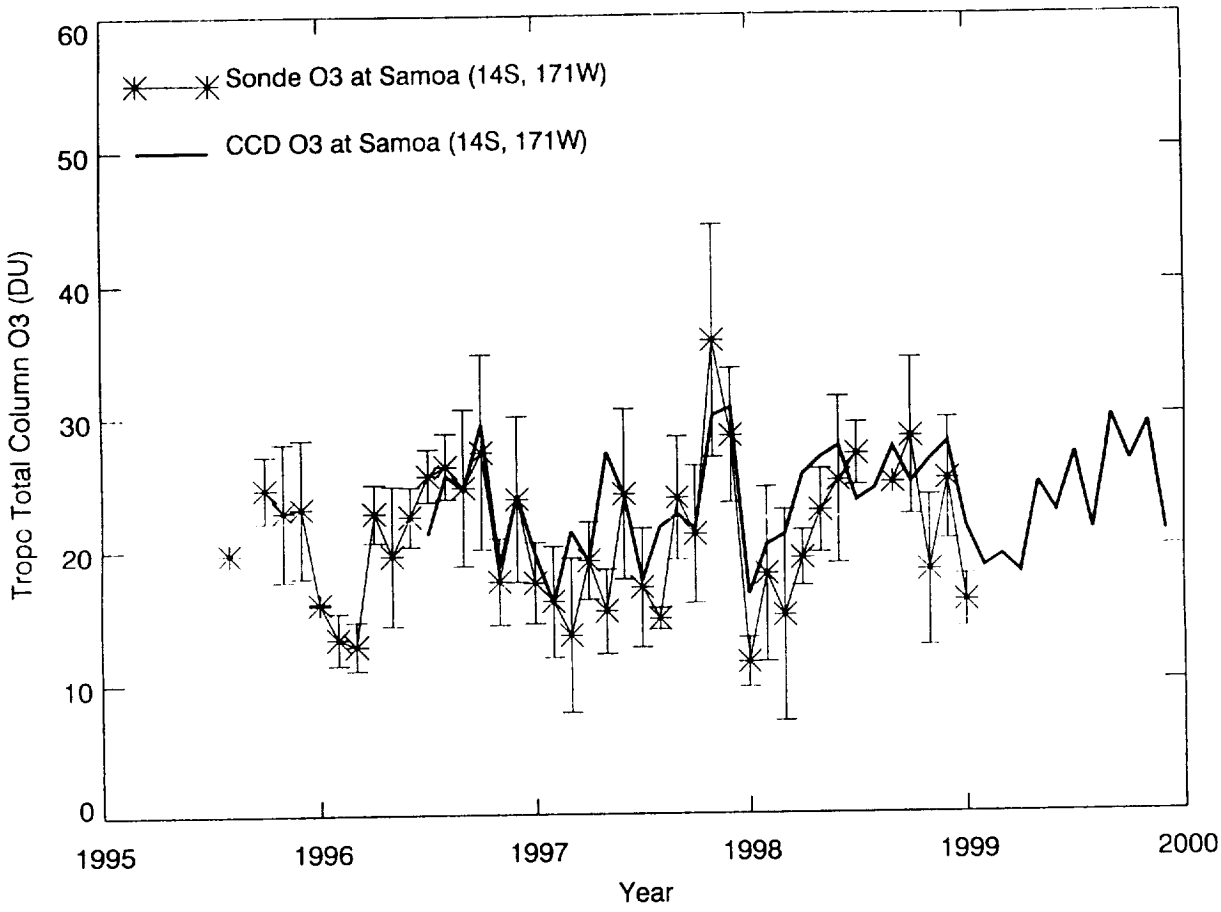

Figure 3. Tropospheric total column O_3 at Samoa (14°S, 171°W) derived from ozonesonde (stars) and CCD method (solid) . Vertical bars for the ozonesonde data represent $\pm 1\sigma$ standard deviations.

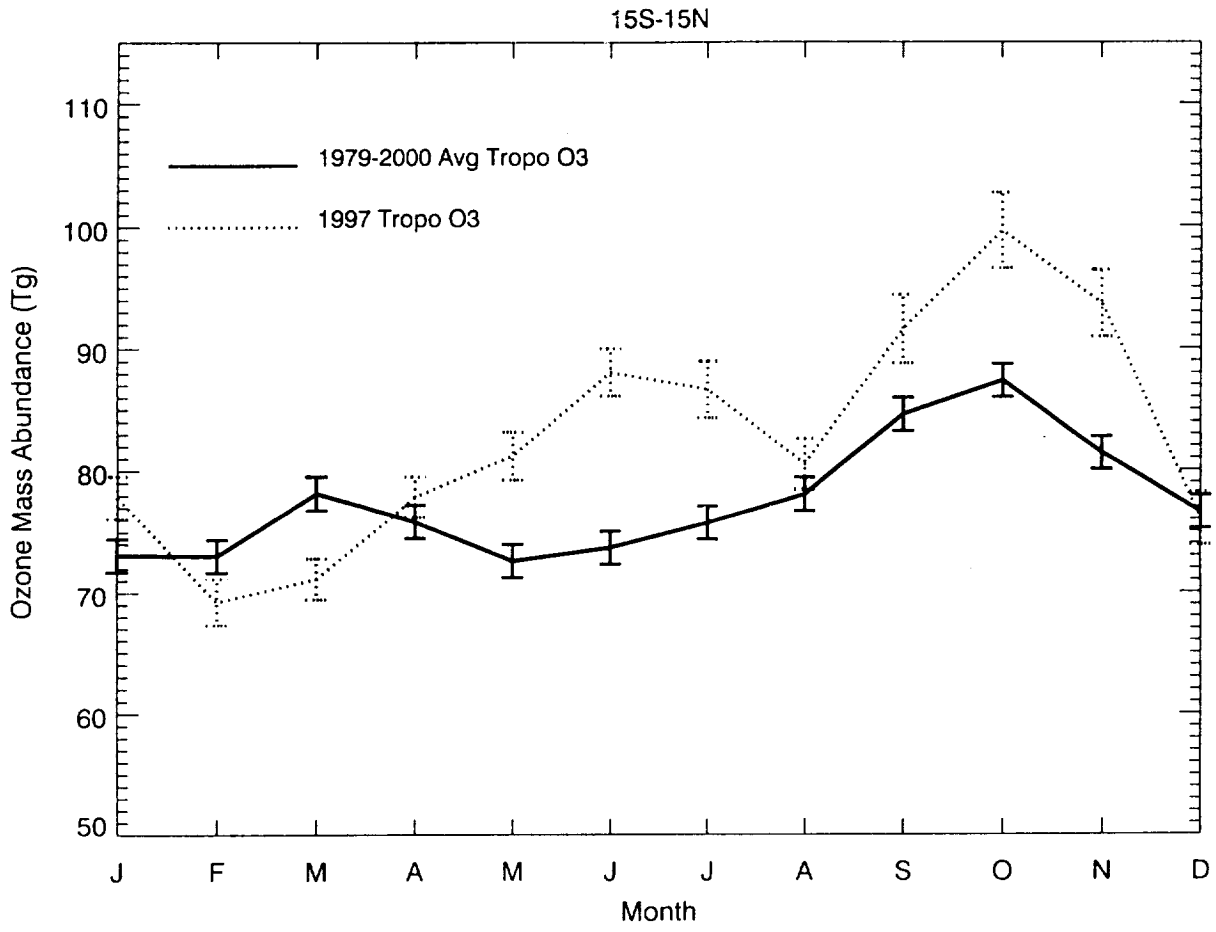

Figure 4. Tropospheric total ozone mass abundance (units Tg) time series derived by area-averaging CCD tropospheric total column O_3 in the latitude band 15°S to 15°N for 1997 (dotted) and a 1979-2000 climatology (solid). Vertical bars represent $\pm 2\sigma$ uncertainties.

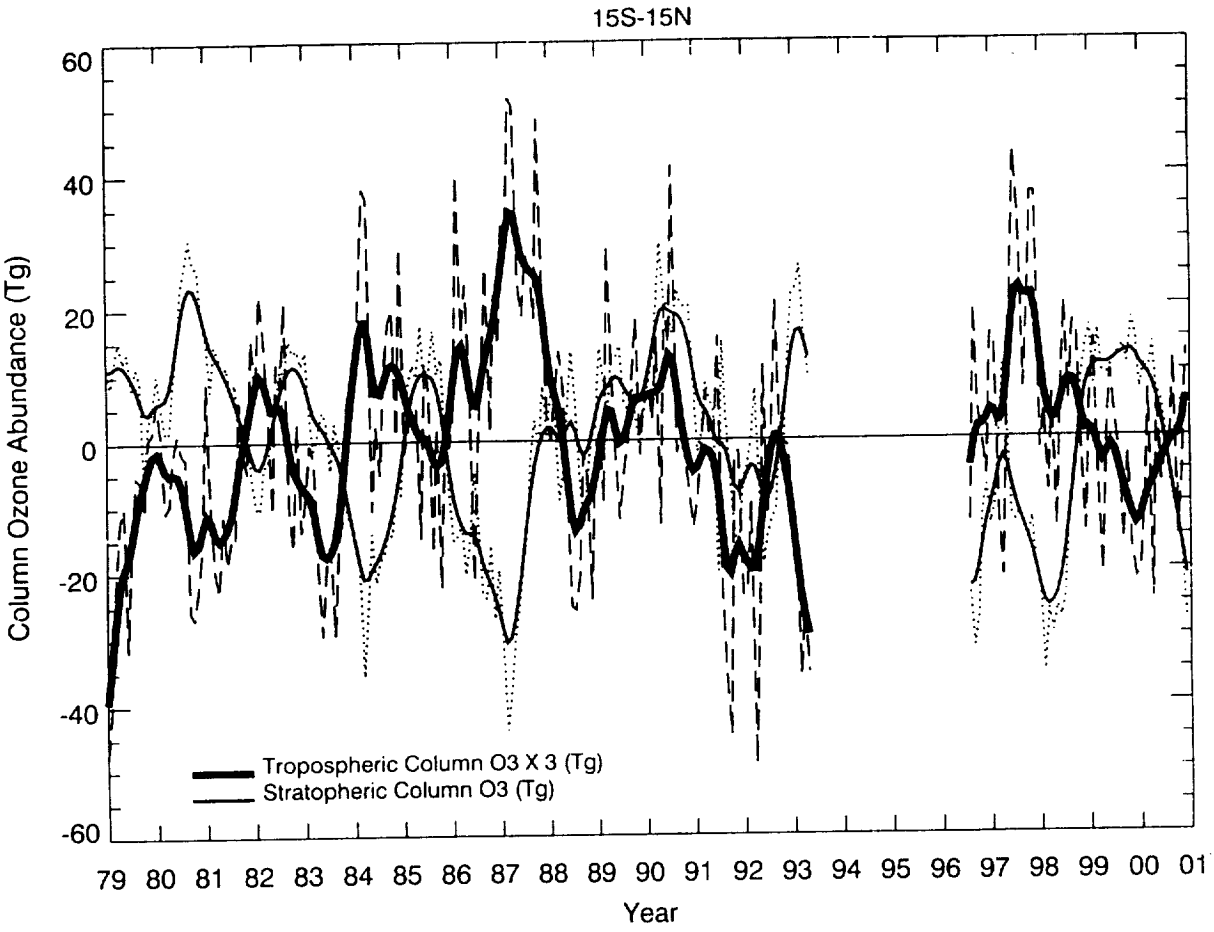

Figure 5. Tropospheric (thick solid) and stratospheric (thin solid) total ozone mass abundance (units Tg) deseasonalized time series derived by area-averaging CCD column O_3 measurements in the latitude band 15°S to 15°N. The original deseasonalized monthly mean data (dotted and dashed curves) were smoothed with a digital recursive low-pass filter with half frequency response at 12-month period.

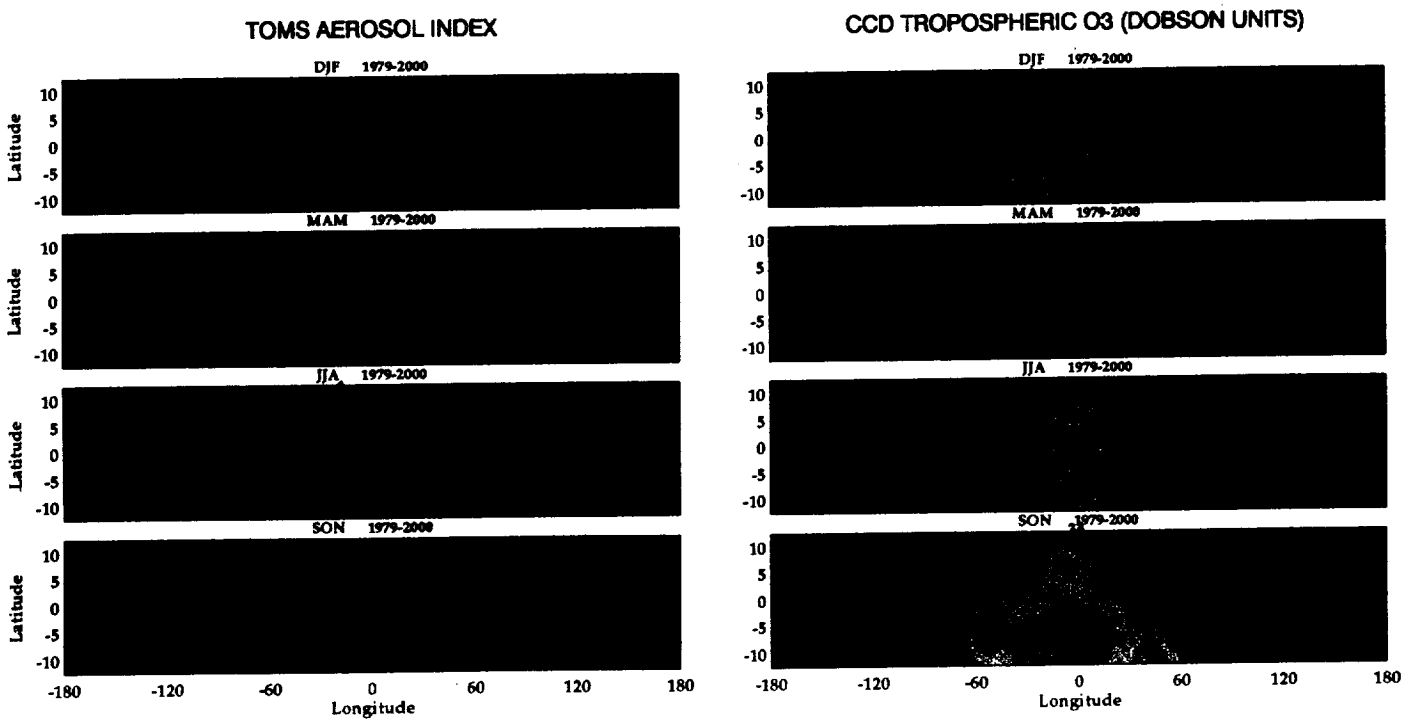

Plate 1. Left: TOMS aerosol index (no units) seasonal climatology. The data shown were determined by averaging over 3-month seasons (indicated) for the time period 1979-2000. Bottom: Same as the left-hand frames, but for TOMS CCD tropospheric total column ozone (in Dobson units).

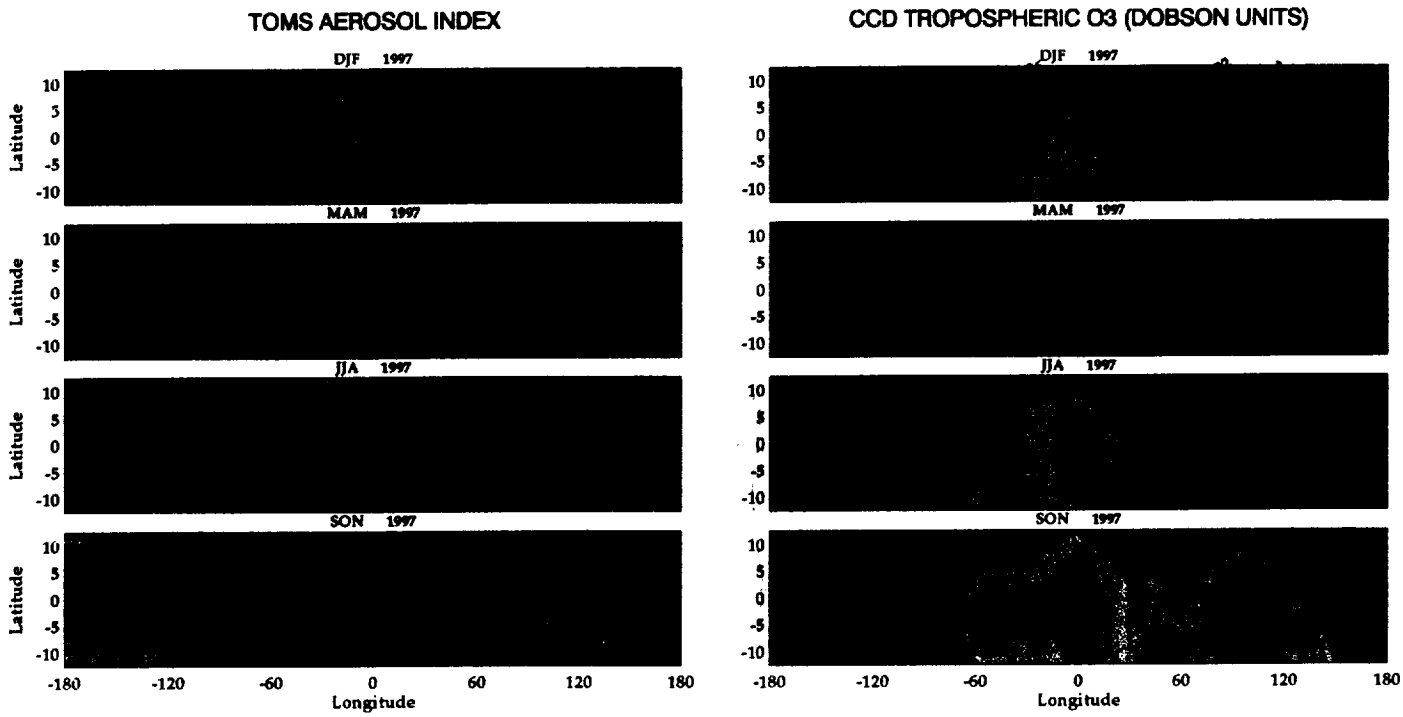

Plate 2. Same as Plate 1, but for the year 1997 instead of climatology.